Letter

Gravitational radiation from inspiralling compact objects: Spin effects to the fourth post-Newtonian order

Gihyuk Cho, Rafael A. Porto, and Zixin Yang
Deutsches Elektronen-Synchrotron DESY, Notkestrasse 85, 22607 Hamburg, Germany

(Received 7 April 2022; accepted 12 October 2022; published 3 November 2022)

The linear- and quadratic-in-spin contributions to the binding potential and gravitational-wave flux from binary systems are derived to next-to-next-to-leading order in the post-Newtonian (PN) expansion of general relativity, including finite-size and tail effects. The calculation is carried out through the worldline effective field theory framework. We find agreement in the overlap with the available PN and self-force literature. As a direct application, we complete the knowledge of spin effects in the evolution of the orbital phase for aligned-spin circular orbits to fourth PN order. We estimate the impact in the number of accumulated gravitational-wave cycles and find they make a significant contribution for next-generation observatories. The results presented here will therefore play an important role in providing reliable physical interpretation of gravitational-wave signals from spinning binaries with future gravitational-wave detectors such as LISA and the Einstein Telescope.

DOI: 10.1103/PhysRevD.106.L101501

I. INTRODUCTION

The dynamical evolution of compact binaries has been the main cause of the gravitational waves (GWs) detected by the LIGO-Virgo-KAGRA interferometers [1–3], and will continue to be one of the primary sources for future GW observatories such as the Laser Interferometer Space Antenna (LISA) [4] and the Einstein Telescope (ET) [5]. The GWs produced by the inspiral, merger, and ring-down from the expected several two-body events will carry vast amounts of information that can shed light on long-standing problems in astrophysics, cosmology, and particle physics [6–9]. In particular the spin of the constituents, which has been found to be large in several recent detections [3], is not only strongly correlated with different formation channels, e.g., [3,10–15], also offers a window to physics beyond the standard model, e.g., [16–24]. Therefore, high-precision waveforms incorporating spin corrections are an essential ingredient to exploit the discovery potential in GW astronomy.

After a concerted effort involving both numerical [25–28] as well as analytic techniques [29–31], GW template banks have been successfully used to analyze the GW data collected thus far [1–3]. However, while current templates may be sufficient for detection, when it comes to parameter estimation, the formidable empirical reach of future experiments require higher levels of accuracy, both for the post-Newtonian (PN) inspiral regime as well as merger stages of the binary's dynamics [32–35].

Presently, although partial results for the derivation of the evolution of the orbital phase in the inspiral regime are known at 4PN order for nonspinning bodies through various computations [36–48], and even higher orders in the conservative sector [49–56], spin contributions have not been pushed so far to the same relative level of accuracy. In particular, for radiative effects, while spin-orbit corrections were obtained to next-to-next-to-leading order (N^2LO) [57,58], complete spin-spin effects are only known to NLO [59–66]. In this paper we fill this gap and report the completion of spin effects to N^2LO in the PN expansion and to quadratic order in the spins, corresponding to the 4PN order for rapidly rotating bodies.

The derivation involves several ingredients, which we obtain using the worldline effective field theory (EFT) framework in the PN regime [67,68] extended to spinning bodies [59–64,69]. The EFT approach uses powerful tools from particle physics resembling, for instance, methodologies used in the calculation of binding energies for heavy quark states [70]. The problem of motion is thus reduced to a series of Feynman diagrams, involving potential and radiation modes, which are constructed by iteratively solving for the (classical) gravitational field sourced by compact objects treated as pointlike objects.

Utilizing the EFT formalism, we have compute the gravitational potential and necessary radiative multipole moments at linear and quadratic order in the spins entering in the flux to N^2LO, including finite-size effects. The completion of spin contributions at 4PN entails also the so-called *tail effect*, due to the scattering of the outgoing radiation off of the background geometry, e.g., [42], which we incorporate through the EFT approach. The values for all of the intermediate (very lengthy) results are displayed in the ancillary file, see also the supplemental material.

 © 2022 American Physical Society

Perfect agreement is found in the overlap with previous results in the literature [57,58,71–79].

From the binding energy and radiated flux we derive the imprint of spin effects in the orbital phase evolution for aligned-spins circular orbits. As a measure of the impact of the new terms, we estimate the accumulated GW cycles for various paradigmatic astrophysical configurations as well as detector-sensitivity curves. We find the N^{2}LO spin terms make a significant contribution both in ET and LISA frequency bands. (The effect increases the larger the mass ratio, which coincidentally is expected to correlate with larger spins [13].) This is partially driven by quadratic-in-spin terms carrying information about the inner structure of the compact objects. The results presented here will therefore play an important role in elucidating the origin of binary black holes as well as aiding future discoveries, such as new dark objects [24] or clouds of putative ultralight particles induced by superradiance [16–23], through GW precision data.

II. WORLDLINE EFT APPROACH

The effective action is obtained in the weak-field regime by *solving for* the metric perturbation in the (classical) saddle-point approximation [59,67]. The bodies are described by the *Routhian*,

$$\mathcal{R} = -\sum_{n=1,2}\left(m_n\sqrt{g_{\mu\nu}v_n^\mu v_n^\nu} + \frac{1}{2}\omega_\mu^{ab}S_{nab}v_n^\mu - \frac{C_{\rm ES^2}^{(n)}}{2m_n}\frac{E_{ab}S_n^{ac}S_{nc}{}^b}{\sqrt{v_n^\mu v_{n\mu}}} + \frac{1}{2m_n}R_{deab}S_n^{ab}S_n^{cd}v_n^e v_{nc} + \cdots\right), \tag{1}$$

which serves both as a Lagrangian for the position variables (x_n^α, v_n^α) and a Hamiltonian for the spin, projected onto a locally-flat frame, $S_n^{ab} \equiv e_\mu^a e_\nu^b S_n^{\mu\nu}$, and coupled to ω_μ^{ab}, the Ricci rotation coefficients. The free parameters include the masses, m_n, as well as $C_{\rm ES^2}^{(n)}$, which accounts for finite-size effects [59–62]. The latter couple to E_{ab}, the electric component of the Weyl tensor. The last term in (1), involving the Riemann tensor, ensures the covariant spin-supplementarity-condition, $S^{ab}v_b = 0$, is preserved upon evolution. However, for convenience, our results will be presented in terms of (Newton-Wigner) precession-only spin variables. The ellipses encapsulate higher orders in spin and curvature, which are not relevant in this paper. See [31] for more details.

III. GRAVITATIONAL POTENTIAL AND BINDING ENERGY

The derivation of the potential follows by computing the "vacuum-to-vacuum" amplitude in the presence of external sources, by *integrating out* the off-shell quasi-instantaneous modes of the gravitational field. The associated Feynman diagrams needed to N^{2}LO are

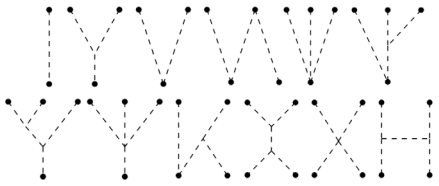

FIG. 1. Topologies needed for the N^{2}LO potential (see text).

depicted in Fig. 1. The worldline couplings, depicted as a black disc, include the mass as well as the linear and quadratic spin terms shown in (1). The dashed lines represent the potential modes of the gravitational field responsible for the binding of the two-body system. Hence, the Green's function (a.k.a. propagator) must be PN expanded [67]

$$\frac{i}{(k^0)^2 - \boldsymbol{k}^2} = -\frac{i}{\boldsymbol{k}^2}\left(1 + \frac{(k^0)^2}{\boldsymbol{k}^2} + \cdots\right), \tag{2}$$

with each factor of $(k^0)^2$ scaling as v^2. From the gravitational potential, and after transforming to conserved-norm spins, we derive the equations of motion including the spin precession, which are displayed in full glory in the ancillary file. The binding energy becomes

$$E_{\rm SO} = \frac{GM\nu}{r^2}\left[e_3^0 + \frac{1}{2}\left(e_5^0 + \frac{GM}{r}e_5^1\right)\right] + \frac{GM\nu}{4r^2}\left[\frac{1}{2}\left(e_7^0 + \frac{GM}{r}e_7^1\right) + \frac{G^2M^2}{r^2}e_7^2\right], \tag{3}$$

for the spin-orbit terms, and

$$E_{\rm SS} = \frac{G\nu}{4r^3}\left[e_4^0 + \frac{1}{2}e_6^0 + \frac{GM}{r}e_6^1\right] + \frac{G\nu}{16r^3}\left[\frac{1}{2}e_8^0 + \frac{GM}{r}e_8^1 + \frac{7}{2}\frac{G^2M^2}{r^2}e_8^2\right], \tag{4}$$

for spin-spin contribution. The value for the e_j^i PN coefficients are given in the Supplemental Material [80] and ancillary file. We use $M \equiv m_1 + m_2$ for the total mass, $\nu \equiv m_1m_2/M^2$ for the symmetric-mass-ratio and $r \equiv |\boldsymbol{x}_1 - \boldsymbol{x}_2|$ the relative distance, respectively. We use the parameter $\delta \equiv (m_1 - m_2)/M$, and $\kappa_\pm \equiv C_{\rm ES^2}^{(1)} \pm C_{\rm ES^2}^{(2)}$. For the spin variables we use the standard, e.g., [29],

$$\boldsymbol{S} \equiv \boldsymbol{S}_1 + \boldsymbol{S}_2, \qquad \boldsymbol{\Sigma} \equiv M\left(\frac{\boldsymbol{S}_2}{m_2} - \frac{\boldsymbol{S}_1}{m_1}\right). \tag{5}$$

IV. RADIATED FLUX

The emitted power is obtained by matching the one-point function to a long-distance worldline effective theory for the binary system treated as a pointlike object endowed with multipole moments. The action includes, in

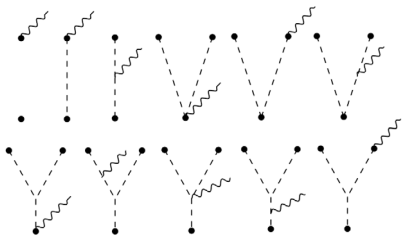

FIG. 2. Topologies needed to match the multipole moments entering the radiated flux to NNLO (see text).

addition to the (Bondi) mass-energy monopole term, $-M_{\rm B}\int d\tau$, a series of symmetric-trace-free (STF) *source* mass, I^L, and current, J^L, time-dependent multipoles, with $L \equiv \{i_1 \cdots i_L\}$, [68]

$$\sum_{\ell=2}\left(\frac{1}{\ell!}I^L_{\rm STF}\nabla_{L-2}\bar{E}_{i_{\ell-1}i_\ell} - \frac{2\ell}{(2\ell+1)!}J^L_{\rm STF}\nabla_{L-2}\bar{B}_{i_{\ell-1}i_\ell}\right), \tag{6}$$

which couple to (covariant) derivatives of $\bar{E}_{ij}$ and $\bar{B}_{kl}$, the electric and magnetic components of the Weyl tensor involving only the *background* radiation field. The relevant topologies are shown in Fig. 2. The wavy line represents the on-shell radiation, which couples both to the constituents of the binary as well as the binding modes. From the source multipoles we compute the energy flux by squaring the emission amplitude [68],

$$\mathcal{F}_{\rm src} = G\left(\frac{1}{5}I^{(3)}_{ij}I^{(3)}_{ij} + \frac{16}{45}J^{(3)}_{ij}J^{(3)}_{ij} + \frac{1}{189}I^{(4)}_{ijk}I^{(4)}_{ijk} + \frac{1}{84}J^{(4)}_{ijk}J^{(4)}_{ijk} + \frac{1}{9072}I^{(5)}_{ijkl}I^{(5)}_{ijkl} + \frac{4}{14175}J^{(5)}_{ijkl}J^{(5)}_{ijkl}\cdots\right), \tag{7}$$

to the desired order. The time derivatives are computed within the adiabatic approximation, by using the conservative equations of motion. We find for the spin-orbit flux,

$$\mathcal{F}^{\rm SO}_{\rm src} = \frac{8G^3M^3\nu^2}{15r^5}\left(\left[f^0_3 + 4\frac{GM}{r}f^1_3\right] + \frac{1}{28}\left[f^0_5 + 2\frac{GM}{r}f^1_5 + 4\frac{G^2M^2}{r^2}f^2_5\right] + \frac{1}{84}\left[f^0_7 + \frac{GM}{r}f^1_7 + \frac{2}{3}\frac{G^2M^2}{r^2}f^2_7 + \frac{4}{9}\frac{G^3M^3}{r^3}f^3_7\right]\right), \tag{8}$$

whereas, for the spin-spin terms we arrive at

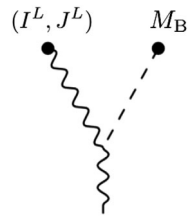

FIG. 3. Tail coupling between the binary's mass monopole and other source moments.

$$\mathcal{F}^{\rm SS}_{\rm src} = \frac{2G^3M^2\nu^2}{15r^6}\left(f^0_4 + \frac{1}{7}\left[f^0_6 + \frac{GM}{r}f^1_6 + 4\frac{G^2M^2}{r^2}f^2_6\right] + \frac{1}{84}\left[f^0_8 + \frac{GM}{r}f^1_8 + \frac{2}{3}\frac{G^2M^2}{r^2}f^2_8 + \frac{8}{3}\frac{G^3M^3}{r^3}f^3_8\right]\right). \tag{9}$$

The value of the f^i_j coefficients are displayed in the Supplemental Material [80] and ancillary file.

In order to complete the derivation of the total flux we must also include the tail effect, depicted in Fig. 3, where the radiated field interacts with the background geometry around the binary system, sourced by the monopole term. This is often packaged in terms of *radiative* multipole moments, which can then be used to compute the total power using (7). The (leading) tail term yields

$$\mathcal{F}_{\rm tail} = -G^2M_{\rm B}\pi\int\left[\left(\frac{2}{5}I_{ij}(p)I_{ij}(q) + \frac{32}{45}J_{ij}(p)J_{ij}(q)\right) - pq\left(\frac{2}{189}I_{ijk}(p)I_{ijk}(q) + \frac{1}{42}J_{ijk}(p)J_{ijk}(q)\right)\right] \times p^3q^4{\rm sign}(q)e^{-i(p+q)t}dpdq, \tag{10}$$

where $I_L(p)$ is the Fourier transform. In the above expression the $M_{\rm B}$ includes not only the total mass of the binary but also the kinetic energy and binding potential to a given PN order.

V. ALIGNED-SPIN CIRCULAR ORBITS

As a direct application of our results we consider the phenomenologically relevant case of (planar) circular orbits with the (conserved-norm) spins being either aligned or antialigned with the angular momentum. In what follow we quote the results using the following projected (dimensionless) spin variables

$$\hat{S}_\ell \equiv \frac{\boldsymbol{\ell}\cdot\boldsymbol{S}}{GM^2}, \qquad \Sigma_\ell \equiv \frac{\boldsymbol{\ell}\cdot\boldsymbol{\Sigma}}{GM^2}, \tag{11}$$

with $\boldsymbol{\ell}$ the unit vector in the direction of the angular momentum. Garnering the pieces together we find

$$
\begin{aligned}
E_{\rm spin} = &-\frac{M\nu x}{2}\left[x^{3/2}\left(\frac{14}{3}\hat{S}_\ell + 2\delta\hat{\Sigma}_\ell\right) + x^2\left\{(-2-\kappa_+)\hat{S}_\ell^2 + [\kappa_- + \delta(-2-\kappa_+)]\hat{S}_\ell\hat{\Sigma}_\ell\right.\right.\\
&\left.\left. + \left[2\nu + \frac{1}{2}\delta\kappa_- + \left(-\frac{1}{2}+\nu\right)\kappa_+\right]\hat{\Sigma}_\ell^2\right\} + x^{5/2}\left[\left(11-\frac{61}{9}\nu\right)\hat{S}_\ell + \left(3-\frac{10}{3}\nu\right)\delta\hat{\Sigma}_\ell\right]\right.\\
&+ x^3\left(\left[\frac{50}{9}+\frac{5}{3}\nu-\frac{5}{3}\delta\kappa_- + \left(-\frac{25}{6}+\frac{5}{6}\nu\right)\kappa_+\right]\hat{S}_\ell^2 + \left\{\left(\frac{5}{2}+\frac{35}{6}\nu\right)\kappa_- + \delta\left[\frac{25}{3}+\frac{5}{3}\nu+\left(-\frac{5}{2}+\frac{5}{6}\nu\right)\kappa_+\right]\right\}\hat{S}_\ell\hat{\Sigma}_\ell\right.\\
&\left.+ \left[5-10\nu-\frac{5}{3}\nu^2 + \left(\frac{5}{4}+\frac{5}{4}\nu\right)\delta\kappa_- + \left(-\frac{5}{4}+\frac{5}{4}\nu-\frac{5}{6}\nu^2\right)\kappa_+\right]\hat{\Sigma}_\ell^2\right)\\
&+ x^{7/2}\left[\left(\frac{135}{4}-\frac{367}{4}\nu+\frac{29}{12}\nu^2\right)\hat{S}_\ell + \left(\frac{27}{4}-39\nu+\frac{5}{4}\nu^2\right)\delta\hat{\Sigma}_\ell\right]\\
&+ x^4\left(\left[\frac{67}{12}+\frac{6445}{108}\nu-\frac{7}{36}\nu^2 + \left(-\frac{31}{4}+\frac{35}{18}\nu\right)\delta\kappa_- + \left(-\frac{125}{8}+\frac{1025}{72}\nu-\frac{7}{72}\nu^2\right)\kappa_+\right]\hat{S}_\ell^2\right.\\
&+ \left\{\left(\frac{63}{8}+\frac{449}{24}\nu-\frac{553}{72}\nu^2\right)\kappa_- + \delta\left[\frac{49}{4}+\frac{1649}{36}\nu-\frac{7}{36}\nu^2 + \left(-\frac{63}{8}+\frac{295}{24}\nu-\frac{7}{72}\nu^2\right)\kappa_+\right]\right\}\hat{S}_\ell\hat{\Sigma}_\ell\\
&\left.\left.+ \left[\frac{21}{2}-\frac{119}{12}\nu-\frac{135}{4}\nu^2+\frac{7}{36}\nu^3 + \left(\frac{63}{16}+\frac{77}{48}\nu-\frac{91}{48}\nu^2\right)\delta\kappa_- + \left(-\frac{63}{16}+\frac{301}{48}\nu-\frac{499}{48}\nu^2+\frac{7}{72}\nu^3\right)\kappa_+\right]\hat{\Sigma}_\ell^2\right)\right], \qquad (12)
\end{aligned}
$$

for the spin-dependent linear- and bilinear-in-spin binding energy as a function of the orbital frequency, $x \equiv (GM\Omega)^{2/3}$, which agrees with the derivations in [72]. On the other hand, the newly computed energy flux becomes

$$
\begin{aligned}
\mathcal{F}_{\rm spin} = &\frac{32\nu^2x^5}{5G}\left[x^{3/2}\left(-4\hat{S}_\ell - \frac{5}{4}\delta\hat{\Sigma}_\ell\right) + x^2\left\{(4+2\kappa_+)\hat{S}_\ell^2 + [-2\kappa_- + \delta(4+2\kappa_+)]\hat{S}_\ell\hat{\Sigma}_\ell\right.\right.\\
&\left.\left. + \left[\frac{1}{16} - 4\nu - \delta\kappa_- + \kappa_+(1-2\nu)\right]\hat{\Sigma}_\ell^2\right\} + x^{5/2}\left[\left(-\frac{9}{2}+\frac{272}{9}\nu\right)\hat{S}_\ell + \delta\left(-\frac{13}{16}+\frac{43}{4}\nu\right)\hat{\Sigma}_\ell\right]\right.\\
&+ x^3\left(-16\pi\hat{S}_\ell - \frac{31}{6}\pi\delta\hat{\Sigma}_\ell + \left[-\frac{5239}{504}-\frac{43}{2}\nu+\frac{41}{16}\delta\kappa_- + \kappa_+\left(-\frac{271}{112}-\frac{43}{4}\nu\right)\right]\hat{S}_\ell^2\right.\\
&+ \left\{\delta\left[-\frac{817}{56}+\kappa_+\left(-\frac{279}{56}-\frac{43}{4}\nu\right)-\frac{43}{2}\nu\right] + \kappa_-\left(\frac{279}{56}+\frac{1}{2}\nu\right)\right\}\hat{S}_\ell\hat{\Sigma}_\ell\\
&\left.+ \left[-\frac{25}{8}+\frac{344}{21}\nu+\frac{43}{2}\nu^2 + \delta\kappa_-\left(\frac{279}{112}+\frac{45}{16}\nu\right) + \kappa_+\left(-\frac{279}{112}+\frac{243}{112}\nu+\frac{43}{4}\nu^2\right)\right]\hat{\Sigma}_\ell^2\right)\\
&+ x^{7/2}\left\{\left(\frac{476645}{6804}+\frac{6172}{189}\nu-\frac{2810}{27}\nu^2\right)\hat{S}_\ell + \delta\left(\frac{9535}{336}+\frac{1849}{126}\nu-\frac{1501}{36}\nu^2\right)\hat{\Sigma}_\ell + (16\pi+8\pi\kappa_+)\hat{S}_\ell^2\right.\\
&+ [-8\pi\kappa_- + \delta(16\pi+8\pi\kappa_+)]\hat{S}_\ell\hat{\Sigma}_\ell + \left.\left[\frac{1}{8}\pi - 4\pi\delta\kappa_- - 16\pi\nu + \kappa_+(4\pi-8\pi\nu)\right]\hat{\Sigma}_\ell^2\right\}\\
&+ x^4\left(\left(-\frac{3485\pi}{96}+\frac{13879\pi}{72}\nu\right)\hat{S}_\ell + \delta\left(-\frac{7163\pi}{672}+\frac{130583\pi}{2016}\nu\right)\hat{\Sigma}_\ell + \left[-\frac{4289}{648}-\frac{295}{21}\nu+54\nu^2 + \delta\kappa_-\left(\frac{935}{336}-\frac{2153}{144}\nu\right)\right.\right.\\
&\left.+ \kappa_+\left(-\frac{124577}{9072}+\frac{3265}{126}\nu+27\nu^2\right)\right]\hat{S}_\ell^2 + \left\{\kappa_-\left(\frac{74911}{4536}-\frac{52411}{1008}\nu+\frac{1181}{36}\nu^2\right)\right.\\
&\left.+ \delta\left[-\frac{160621}{9072}+\frac{9977}{252}\nu+54\nu^2 + \kappa_+\left(-\frac{74911}{4536}+\frac{41191}{1008}\nu+27\nu^2\right)\right]\right\}\hat{S}_\ell\hat{\Sigma}_\ell\\
&+ \left[\frac{1633}{336}+\frac{465071}{18144}\nu-\frac{74033}{1008}\nu^2-54\nu^3 + \delta\kappa_-\left(\frac{74911}{9072}-\frac{46801}{2016}\nu+\frac{209}{144}\nu^2\right)\right.\\
&\left.\left.+ \kappa_+\left(-\frac{74911}{9072}+\frac{102979}{2592}\nu-\frac{7109}{168}\nu^2-27\nu^3\right)\right]\hat{\Sigma}_\ell^2\right)\Bigg]. \qquad (13)
\end{aligned}
$$

As a consistency check, this result agrees to the given PN order with the GW flux for a nonspinning test body orbiting around a Kerr black hole, as well as for a body with spin aligned to the angular momentum in a Schwarzschild background to first order in the mass-ratio, computed in [78,79] respectively.

We then combine these results to derive the evolution of the orbital frequency, from which we infer the change in the orbital phase, $\phi = \int \Omega(t) dt$, using the TaylorT2 approximant, e.g., [32], yielding

$$
\begin{aligned}
\phi_{\rm spin} = -\frac{x^{-5/2}}{32\nu}\Bigg[& x^{3/2}\left(\frac{235}{6}\hat{S}_\ell + \frac{125}{8}\delta\hat{\Sigma}_\ell\right) + x^2\Bigg\{(-50-25\kappa_+)\hat{S}_\ell^2 \\
& + [25\kappa_- + \delta(-50-25\kappa_+)]\hat{S}_\ell\hat{\Sigma}_\ell + \left[-\frac{5}{16} + 50\nu + \frac{25}{2}\delta\kappa_- + \left(-\frac{25}{2} + 25\nu\right)\kappa_+\right]\hat{\Sigma}_\ell^2\Bigg\} \\
& + x^{5/2}\log x\left[\left(-\frac{554345}{2016} - \frac{55}{8}\nu\right)\hat{S}_\ell + \left(-\frac{41745}{448} + \frac{15}{8}\nu\right)\delta\hat{\Sigma}_\ell\right] \\
& + x^3\Bigg(\frac{940}{3}\pi\hat{S}_\ell + \frac{745}{6}\pi\delta\hat{\Sigma}_\ell + \left[-\frac{31075}{126} + 60\nu + \frac{2215}{48}\delta\kappa_- + \left(\frac{15635}{84} + 30\nu\right)\kappa_+\right]\hat{S}_\ell^2 \\
& + \left\{\left(-\frac{47035}{336} - \frac{2575}{12}\nu\right)\kappa_- + \delta\left[-\frac{9775}{42} + 60\nu + \left(\frac{47035}{336} + 30\nu\right)\kappa_+\right]\right\}\hat{S}_\ell\hat{\Sigma}_\ell \\
& + \left[-\frac{410825}{2688} + \frac{23535}{112}\nu - 60\nu^2 + \left(-\frac{47035}{672} - \frac{2935}{48}\nu\right)\delta\kappa_- + \left(\frac{47035}{672} - \frac{4415}{56}\nu - 30\nu^2\right)\kappa_+\right]\hat{\Sigma}_\ell^2\Bigg) \\
& + x^{7/2}\Bigg\{\left(-\frac{8980424995}{6096384} + \frac{6586595}{6048}\nu - \frac{305}{288}\nu^2\right)\hat{S}_\ell + \left(-\frac{170978035}{387072} + \frac{2876425}{5376}\nu + \frac{4735}{1152}\nu^2\right)\delta\hat{\Sigma}_\ell \\
& + (-100\pi - 50\pi\kappa_+)\hat{S}_\ell^2 + [50\pi\kappa_- + \delta(-100\pi - 50\pi\kappa_+)]\hat{S}_\ell\hat{\Sigma}_\ell + \left[-\frac{15}{16}\pi + 100\nu\pi + 25\pi\delta\kappa_- + (-25\pi + 50\nu\pi)\kappa_+\right]\hat{\Sigma}_\ell^2\Bigg\} \\
& + x^4\Bigg(\left(\frac{2388425\pi}{3024} - \frac{9925\pi}{36}\nu\right)\hat{S}_\ell + \delta\left(\frac{3237995\pi}{12096} - \frac{258245\pi}{2016}\nu\right)\hat{\Sigma}_\ell \\
& + \left[-\frac{83427805}{72576} - \frac{19720}{63}\nu + \frac{475}{24}\nu^2 + \left(\frac{3284125}{24192} + \frac{1115}{72}\nu\right)\delta\kappa_-\right. \\
& \left. + \left(\frac{55124675}{145152} - \frac{32825}{756}\nu + \frac{475}{48}\nu^2\right)\kappa_+\right]\hat{S}_\ell^2 + \Bigg\{\left(-\frac{35419925}{145152} - \frac{975955}{2016}\nu - \frac{10345}{144}\nu^2\right)\kappa_- \\
& + \delta\left[-\frac{66536845}{72576} - \frac{109535}{378}\nu + \frac{475}{24}\nu^2 + \left(\frac{35419925}{145152} - \frac{89065}{1512}\nu + \frac{475}{48}\nu^2\right)\kappa_+\right]\Bigg\}\hat{S}_\ell\hat{\Sigma}_\ell \\
& + \Bigg[-\frac{17815050265}{48771072} + \frac{26426305}{41472}\nu + \frac{12570535}{48384}\nu^2 - \frac{475}{24}\nu^3 + \left(-\frac{35419925}{290304} - \frac{2571605}{24192}\nu - \frac{5885}{288}\nu^2\right)\delta\kappa_- \\
& + \left(\frac{35419925}{290304} - \frac{19990295}{145152}\nu + \frac{479845}{6048}\nu^2 - \frac{475}{48}\nu^3\right)\kappa_+\Bigg]\hat{\Sigma}_\ell^2\Bigg)\Bigg], \qquad (14)
\end{aligned}
$$

included in the ancillary file for the reader's convenience. We find perfect agreement in the overlap at linear order in the spin to 3.5PN of [58,71], whereas spin-spin effects including finite-size corrections, both at 3.5PN and 4PN orders, are reported here for the first time.

VI. CONCLUSIONS AND OUTLOOK

We have completed the knowledge of spin effects in the orbital phase evolution of compact binary systems to N^{2}LO in the PN expansion of general relativity and quadratic order in the spins, corresponding to an overall 4PN order for rapidly rotating bodies, including both finite-size as well as tail effects. The various ingredients for the full derivation, such as the gravitational potential and multipole moments, were obtained through the worldline EFT framework for spinning compact objects [31], which systematizes the two-body problem into a series of Feynman diagrams involving potential and radiation modes. Agreement is found in the overlap with previous derivations in the conservative [72–77] and radiation sectors [57,58,71,78,79]. Our results here then demonstrate how

the EFT formalism can be pushed to high PN orders, reaching the very state-of-the-art not only in the conservative [45,46,49,50] but also in the radiative regime. In order to estimate the potential impact of the new spin-dependent terms in the GW phase evolution, we used the leading quadrupolar approximation ($\phi_{\rm GW} \simeq 2\phi$) to compute the effect of the different PN terms on the number of GW cycles in future detector's bands operating at design-sensitivity.[1] The results, particularized to LISA (0.1 mHz to $min(f_{\rm ISCO}$, 1 Hz)) and ET (1 Hz to $f_{\rm ISCO}$, with the frequency of the innermost stable circular orbit given by $f_{\rm ISCO} = \frac{1}{6^{3/2}\pi GM}$), are summarized in the following table (see e.g., Table 4 in sec. 11.3 in [29])[2]:

LISA	$10^6 M_\odot + 10 M_\odot$	$10^5 M_\odot + 10 M_\odot$	$10^4 M_\odot + 10^4 M_\odot$
3.5PN	$224615.\hat{S}_\ell + (47903.6 + 23951.8\kappa_+)\hat{S}_\ell^2 + 67352.3\hat{\Sigma}_\ell + (47902.6 - 23951.8\kappa_- + 23951.3\kappa_+)\hat{S}_\ell\hat{\Sigma}_\ell + (448.6 - 11975.6\kappa_- + 11975.6\kappa_+)\hat{\Sigma}_\ell^2$	$24002.2\hat{S}_\ell + (5119.3 + 2559.6\kappa_+)\hat{S}_\ell^2 + 7195.6\hat{\Sigma}_\ell + (5118.2 - 2559.6\kappa_- + 2559.1\kappa_+)\hat{S}_\ell\hat{\Sigma}_\ell + (47.5 - 1279.6\kappa_- + 1279.6\kappa_+)\hat{\Sigma}_\ell^2$	$4.7\hat{S}_\ell + (1.2 + 0.6\kappa_+)\hat{S}_\ell^2 - 0.6\kappa_-\hat{S}_\ell\hat{\Sigma}_\ell + (-0.3 + 0.2\kappa_+)\hat{\Sigma}_\ell^2$
4PN	$-164123.\hat{S}_\ell + (76034.4 - 8979.\kappa_- - 25119.6\kappa_+)\hat{S}_\ell^2 - 55624.3\hat{\Sigma}_\ell + (60639.1 + 16140.8\kappa_- - 16140.1\kappa_+)\hat{S}_\ell\hat{\Sigma}_\ell + (24160.6 + 8070.1\kappa_- - 8070.1\kappa_+)\hat{\Sigma}_\ell^2$	$-16758.5\hat{S}_\ell + (7764.3 - 916.7\kappa_- - 2565.\kappa_+)\hat{S}_\ell^2 - 5678.7\hat{\Sigma}_\ell + (6191.1 + 1648.5\kappa_- - 1647.8\kappa_+)\hat{S}_\ell\hat{\Sigma}_\ell + (2466.7 + 824.\kappa_- - 824.\kappa_+)\hat{\Sigma}_\ell^2$	$-2.8\hat{S}_\ell + (1.5 - 0.4\kappa_+)\hat{S}_\ell^2 + 0.4\kappa_-\hat{S}_\ell\hat{\Sigma}_\ell + (0.2 - 0.1\kappa_+)\hat{\Sigma}_\ell^2$
ET	$100\ M_\odot + 1.4\ M_\odot$	$10 M_\odot + 10 M_\odot$	$10 M_\odot + 1.4 M_\odot$
3.5PN	$163.2\hat{S}_\ell + (35.2 + 17.6\kappa_+)\hat{S}_\ell^2 + 47.3\hat{\Sigma}_\ell + (34.2 - 17.6\kappa_- + 17.1\kappa_+)\hat{S}_\ell\hat{\Sigma}_\ell + (-0.1 - 8.5\kappa_- + 8.5\kappa_+)\hat{\Sigma}_\ell^2$	$7.7\hat{S}_\ell + (2. + \kappa_+)\hat{S}_\ell^2 - \kappa_-\hat{S}_\ell\hat{\Sigma}_\ell + (-0.5 + 0.2\kappa_+)\hat{\Sigma}_\ell^2$	$20.5\hat{S}_\ell + (4.7 + 2.4\kappa_+)\hat{S}_\ell^2 + 4.4\hat{\Sigma}_\ell + (3.6 - 2.4\kappa_- + 1.8\kappa_+)\hat{S}_\ell\hat{\Sigma}_\ell + (-0.5 - 0.9\kappa_- + 0.9\kappa_+)\hat{\Sigma}_\ell^2$
4PN	$-119.9\hat{S}_\ell + (56 - 6.4\kappa_- - 18.4\kappa_+)\hat{S}_\ell^2 - 39.4\hat{\Sigma}_\ell + (43.5 + 12.2\kappa_- - 11.5\kappa_+)\hat{S}_\ell\hat{\Sigma}_\ell + (17.3 + 5.8\kappa_- - 5.8\kappa_+)\hat{\Sigma}_\ell^2$	$-6.1\hat{S}_\ell + (3.3 - \kappa_+)\hat{S}_\ell^2 + \kappa_-\hat{S}_\ell\hat{\Sigma}_\ell + (0.5 - 0.2\kappa_+)\hat{\Sigma}_\ell^2$	$-15.\hat{S}_\ell + (7.4 - 0.6\kappa_- - 2.4\kappa_+)\hat{S}_\ell^2 - 3.8\hat{\Sigma}_\ell + (4.5 + 1.9\kappa_- - 1.1\kappa_+)\hat{S}_\ell\hat{\Sigma}_\ell + (1.8 + 0.6\kappa_- - 0.7\kappa_+)\hat{\Sigma}_\ell^2$

Although generically relevant for comparable masses, spin effects become more important for binaries with unequal masses, which are also expected to exhibit larger spins [13]. Moreover, terms depending on the inner structure of compact bodies and nearby surroundings through the $\kappa_\pm$ couplings [17,18] account for a large portion of the GW cycles for third-generation detectors. We thus expect that N^{2}LO spin terms will play an important role in providing accurate waveform models and reliable interpretation of future GW signals from rotating compact binaries. The results presented here thus motivate further in-depth studies, e.g., extending the effective-one-body analysis in [81] (which included only conservative spin terms [72]), to fully characterize their impact for next-generation GW experiments.

[1]Since we focus on next-generation detectors, for which the inspiral phase is expected to capture a large portion of the observed cycles, our PN derivation should serve as a relatively good estimate once all regimes are included in the analysis, e.g., [81–83].

[2]We have not included the known absorption [84–86], radiation-reaction [87,88] or cubic-in-spin [89] effects.

ACKNOWLEDGMENTS

We are grateful to Brian Pardo for collaboration in [66] and during the early stages of this project. We thank Gregor Kälin for his help drawing the diagrams. This work was supported by the ERC Consolidator Grant "Precision Gravity: From the LHC to LISA," provided by the European Research Council (ERC) under the European Union's H2020 research and innovation programme, Grant No. 817791. We acknowledge extensive use of the xAct packages [90].

[1] R. Abbott *et al.* (LIGO Scientific, VIRGO, and KAGRA Collaborations), GWTC-3: Compact binary coalescences observed by LIGO and Virgo during the second part of the third observing run, arXiv:2111.03606.

[2] A. H. Nitz, S. Kumar, Y.-F. Wang, S. Kastha, S. Wu, M. Schäfer, R. Dhurkunde, and C. D. Capano, 4-OGC: Catalog of gravitational waves from compact-binary mergers, arXiv:2112.06878.

[3] S. Olsen, T. Venumadhav, J. Mushkin, J. Roulet, B. Zackay, and M. Zaldarriaga, New binary black hole mergers in the LIGO–Virgo O3a data, Phys. Rev. D **106**, 043009 (2022).

[4] P. Amaro-Seoane *et al.* (LISA Collaboration), Laser interferometer space antenna, arXiv:1702.00786.

[5] M. Punturo *et al.*, The einstein telescope: A third-generation gravitational wave observatory, Classical Quantum Gravity **27**, 194002 (2010).

[6] R. A. Porto, The tune of Love and the nature(ness) of spacetime, Fortschr. Phys. **64**, 723 (2016).
[7] R. A. Porto, The music of the spheres: The dawn of gravitational wave science, arXiv:1703.06440.
[8] M. Maggiore *et al.*, Science case for the Einstein telescope, J. Cosmol. Astropart. Phys. 03 (2020) 050.
[9] R. Alves Batista *et al.*, EuCAPT white paper: Opportunities and challenges for theoretical astroparticle physics in the next decade, arXiv:2110.10074.
[10] D. Kushnir, M. Zaldarriaga, J. A. Kollmeier, and R. Waldman, GW150914: Spin based constraints on the merger time of the progenitor system, Mon. Not. R. Astron. Soc. **462**, 844 (2016).
[11] W. M. Farr, S. Stevenson, M. Coleman Miller, I. Mandel, B. Farr, and A. Vecchio, Distinguishing spin-aligned and isotropic black hole populations with gravitational waves, Nature (London) **548**, 426 (2017).
[12] J. Roulet, H. S. Chia, S. Olsen, L. Dai, T. Venumadhav, B. Zackay, and M. Zaldarriaga, Distribution of effective spins and masses of binary black holes from the LIGO and Virgo O1–O3a observing runs, Phys. Rev. D **104**, 083010 (2021).
[13] T. A. Callister, C.-J. Haster, K. K. Y. Ng, S. Vitale, and W. M. Farr, Who ordered that? Unequal-mass binary black hole mergers have larger effective spins, Astrophys. J. Lett. **922**, L5 (2021).
[14] Y. Bouffanais, M. Mapelli, F. Santoliquido, N. Giacobbo, U. N. Di Carlo, S. Rastello, M. C. Artale, and G. Iorio, New insights on binary black hole formation channels after GWTC-2: Young star clusters versus isolated binaries, Mon. Not. R. Astron. Soc. **507**, 5224 (2021).
[15] G. Franciolini, R. Cotesta, N. Loutrel, E. Berti, P. Pani, and A. Riotto, How to assess the primordial origin of single gravitational-wave events with mass, spin, eccentricity, and deformability measurements, Phys. Rev. D **105**, 063510 (2022).
[16] A. Arvanitaki and S. Dubovsky, Exploring the string axiverse with precision black hole physics, Phys. Rev. D **83**, 044026 (2011).
[17] D. Baumann, H. S. Chia, and R. A. Porto, Probing ultralight bosons with binary black holes, Phys. Rev. D **99**, 044001 (2019).
[18] D. Baumann, H. S. Chia, R. A. Porto, and J. Stout, Gravitational collider physics, Phys. Rev. D **101**, 083019 (2020).
[19] S. Vitale, R. Lynch, J. Veitch, V. Raymond, and R. Sturani, Measuring the Spin of Black Holes in Binary Systems Using Gravitational Waves, Phys. Rev. Lett. **112**, 251101 (2014).
[20] K. K. Ng, M. Isi, C.-J. Haster, and S. Vitale, Multiband gravitational-wave searches for ultralight bosons, Phys. Rev. D **102**, 083020 (2020).
[21] R. Abbott *et al.* (LIGO Scientific, VIRGO, and KAGRA Collaborations), All-sky search for gravitational wave emission from scalar boson clouds around spinning black holes in LIGO O3 data, Phys. Rev. D **105**, 102001 (2022).
[22] Q. Ding, X. Tong, and Y. Wang, Gravitational collider physics via pulsar-black hole binaries, Astrophys. J. **908**, 78 (2021).
[23] T. Takahashi and T. Tanaka, Axion clouds may survive the perturbative tidal interaction over the early inspiral phase of black hole binaries, J. Cosmol. Astropart. Phys. 10 (2021) 031.
[24] E. Maggio, P. Pani, and G. Raposo, Testing the nature of dark compact objects with gravitational waves, *Handbook of Gravitational Wave Astronomy*, edited by C. Bambi, S. Katsanevas, and K. D. Kokkotas (Springer, Singapore, 2021), 10.1007/978-981-15-4702-7_29-1.
[25] P. Ajith *et al.*, The NINJA-2 catalog of hybrid post-Newtonian/numerical-relativity waveforms for non-precessing black-hole binaries, Classical Quantum Gravity **29**, 124001 (2012); Erratum, Classical Quantum Gravity **30**, 199401 (2013).
[26] B. Szilágyi, J. Blackman, A. Buonanno, A. Taracchini, H. P. Pfeiffer, M. A. Scheel, T. Chu, L. E. Kidder, and Y. Pan, Approaching the Post-Newtonian Regime with Numerical Relativity: A Compact-Object Binary Simulation Spanning 350 Gravitational-Wave Cycles, Phys. Rev. Lett. **115**, 031102 (2015).
[27] T. Dietrich, D. Radice, S. Bernuzzi, F. Zappa, A. Perego, B. Brügmann, S. V. Chaurasia, R. Dudi, W. Tichy, and M. Ujevic, CoRe database of binary neutron star merger waveforms, Classical Quantum Gravity **35**, 24LT01 (2018).
[28] L. Barack and A. Pound, Self-force and radiation reaction in general relativity, Rep. Prog. Phys. **82**, 016904 (2019).
[29] L. Blanchet, Gravitational radiation from post-Newtonian sources and inspiralling compact binaries, Living Rev. Relativity **17**, 2 (2014).
[30] G. Schäfer and P. Jaranowski, Hamiltonian formulation of general relativity and post-Newtonian dynamics of compact binaries, Living Rev. Relativity **21**, 7 (2018).
[31] R. A. Porto, The effective field theorist's approach to gravitational dynamics, Phys. Rep. **633**, 1 (2016).
[32] A. Buonanno, B. Iyer, E. Ochsner, Y. Pan, and B. S. Sathyaprakash, Comparison of post-Newtonian templates for compact binary inspiral signals in gravitational-wave detectors, Phys. Rev. D **80**, 084043 (2009).
[33] M. Pürrer and C.-J. Haster, Gravitational waveform accuracy requirements for future ground-based detectors, Phys. Rev. Res. **2**, 023151 (2020).
[34] D. Ferguson, K. Jani, P. Laguna, and D. Shoemaker, Assessing the readiness of numerical relativity for LISA and 3G detectors, Phys. Rev. D **104**, 044037 (2021).
[35] S. Galaudage, C. Talbot, T. Nagar, D. Jain, E. Thrane, and I. Mandel, Building better spin models for merging binary black holes: Evidence for nonspinning and rapidly spinning nearly aligned subpopulations, Astrophys. J. Lett. **921**, L15 (2021).
[36] T. Damour, P. Jaranowski, and G. Schäfer, Nonlocal-in-time action for the fourth post-Newtonian conservative dynamics of two-body systems, Phys. Rev. D **89**, 064058 (2014).
[37] P. Jaranowski and G. Schäfer, Derivation of local-in-time fourth post-Newtonian ADM Hamiltonian for spinless compact binaries, Phys. Rev. D **92**, 124043 (2015).
[38] L. Bernard, L. Blanchet, A. Bohe, G. Faye, and S. Marsat, Fokker action of nonspinning compact binaries at the fourth post-Newtonian approximation, Phys. Rev. D **93**, 084037 (2016).
[39] L. Bernard, L. Blanchet, A. Bohe, G. Faye, and S. Marsat, Dimensional regularization of the IR divergences in the Fokker action of point-particle binaries at the fourth post-Newtonian order, Phys. Rev. D **96**, 104043 (2017).

[40] T. Marchand, L. Bernard, L. Blanchet, and G. Faye, Ambiguity-free completion of the equations of motion of compact binary systems at the fourth post-Newtonian order, Phys. Rev. D **97**, 044023 (2018).
[41] D. Bini, T. Damour, and A. Geralico, Novel Approach to Binary Dynamics: Application to the Fifth Post-Newtonian Level, Phys. Rev. Lett. **123**, 231104 (2019).
[42] C. Galley, A. Leibovich, R. A. Porto, and A. Ross, Tail effect in gravitational radiation reaction: Time nonlocality and renormalization group evolution, Phys. Rev. D **93**, 124010 (2016).
[43] R. A. Porto and I. Rothstein, Apparent ambiguities in the post-Newtonian expansion for binary systems, Phys. Rev. D **96**, 024062 (2017).
[44] R. A. Porto, Lamb shift and the gravitational binding energy for binary black holes, Phys. Rev. D **96**, 024063 (2017).
[45] S. Foffa and R. Sturani, Dynamics of the gravitational two-body problem at fourth post-Newtonian order and at quadratic order in the Newton constant, Phys. Rev. D **87**, 064011 (2013).
[46] S. Foffa, R. A. Porto, I. Rothstein, and R. Sturani, Conservative dynamics of binary systems to fourth Post-Newtonian order in the EFT approach II: Renormalized Lagrangian, Phys. Rev. D **100**, 024048 (2019).
[47] T. Marchand, Q. Henry, F. Larrouturou, S. Marsat, G. Faye, and L. Blanchet, The mass quadrupole moment of compact binary systems at the fourth post-Newtonian order, Classical Quantum Gravity **37**, 215006 (2020).
[48] Q. Henry, G. Faye, and L. Blanchet, The current-type quadrupole moment and gravitational-wave mode $(\ell, \mathrm{m}) = (2, 1)$ of compact binary systems at the third post-Newtonian order, Classical Quantum Gravity **38**, 185004 (2021).
[49] J. Blümlein, A. Maier, P. Marquard, and G. Schäfer, The fifth-order post-Newtonian Hamiltonian dynamics of two-body systems from an effective field theory approach: Potential contributions, Nucl. Phys. **B965**, 115352 (2021).
[50] J. Blümlein, A. Maier, P. Marquard, and G. Schäfer, The fifth-order post-Newtonian Hamiltonian dynamics of two-body systems from an effective field theory approach, Nucl. Phys. **B983**, 115900 (2022).
[51] S. Foffa and R. Sturani, Hereditary terms at next-to-leading order in two-body gravitational dynamics, Phys. Rev. D **101**, 064033 (2020).
[52] G. L. Almeida, S. Foffa, and R. Sturani, Tail contributions to gravitational conservative dynamics, Phys. Rev. D **104**, 124075 (2021).
[53] J. Blümlein, A. Maier, P. Marquard, and G. Schäfer, Testing binary dynamics in gravity at the sixth post-Newtonian level, Phys. Lett. B **807**, 135496 (2020).
[54] J. Blümlein, A. Maier, P. Marquard, and G. Schäfer, The 6th post-Newtonian potential terms at $O(G_N^4)$, Phys. Lett. B **816**, 136260 (2021).
[55] D. Bini, T. Damour, and A. Geralico, Sixth post-Newtonian local-in-time dynamics of binary systems, Phys. Rev. D **102**, 024061 (2020).
[56] D. Bini, T. Damour, and A. Geralico, Sixth post-Newtonian nonlocal-in-time dynamics of binary systems, Phys. Rev. D **102**, 084047 (2020).
[57] S. Marsat, A. Bohe, G. Faye, and L. Blanchet, Next-to-next-to-leading order spin-orbit effects in the equations of motion of compact binary systems, Classical Quantum Gravity **30**, 055007 (2013).
[58] A. Bohé, S. Marsat, and L. Blanchet, Next-to-next-to-leading order spin–orbit effects in the gravitational wave flux and orbital phasing of compact binaries, Classical Quantum Gravity **30**, 135009 (2013).
[59] R. A. Porto, Post-Newtonian corrections to the motion of spinning bodies in NRGR, Phys. Rev. D **73**, 104031 (2006).
[60] R. A. Porto and I. Z. Rothstein, The Hyperfine Einstein-Infeld-Hoffmann Potential, Phys. Rev. Lett. **97**, 021101 (2006).
[61] R. A. Porto and I. Rothstein, Spin(1)Spin(2) effects in the motion of inspiralling compact binaries at third order in the post-Newtonian expansion, Phys. Rev. D **78**, 044012 (2008); Erratum, Phys. Rev. D **81**, 029904 (2010).
[62] R. A. Porto and I. Z. Rothstein, Next to leading order Spin (1)Spin(1) effects in the motion of inspiralling compact binaries, Phys. Rev. D **78**, 044013 (2008).
[63] R. A. Porto, A. Ross, and I. Z. Rothstein, Spin induced multipole moments for the gravitational wave flux from binary inspirals to third post-Newtonian order, J. Cosmol. Astropart. Phys. 03 (2011) 009.
[64] R. A. Porto, A. Ross, and I. Z. Rothstein, Spin induced multipole moments for the gravitational wave amplitude from binary inspirals to 2.5 Post-Newtonian order, J. Cosmol. Astropart. Phys. 09 (2012) 028.
[65] A. Bohé, Alejandro, G. Faye, S. Marsat, and E. K. Porter, Quadratic-in-spin effects in the orbital dynamics and gravitational-wave energy flux of compact binaries at the 3PN order, Classical Quantum Gravity **32**, 195010 (2015).
[66] G. Cho, B. Pardo, and R. A. Porto, Gravitational radiation from inspiralling compact objects: Spin-spin effects completed at the next-to-leading post-Newtonian order, Phys. Rev. D **104**, 024037 (2021).
[67] W. D. Goldberger and I. Z. Rothstein, An effective field theory of gravity for extended objects, Phys. Rev. D **73**, 104029 (2006).
[68] W. D. Goldberger and A. Ross, Gravitational radiative corrections from effective field theory, Phys. Rev. D **81**, 124015 (2010).
[69] R. A. Porto, Next-to-leading order spin-orbit effects in the motion of inspiralling compact binaries, Classical Quantum Gravity **27**, 205001 (2010).
[70] I. Z. Rothstein, TASI lectures on effective field theories, arXiv:hep-ph/0308266.
[71] S. Marsat, A. Bohé, L. Blanchet, and A. Buonanno, Next-to-leading tail-induced spin–orbit effects in the gravitational radiation flux of compact binaries, Classical Quantum Gravity **31**, 025023 (2014).
[72] M. Levi and J. Steinhoff, Complete conservative dynamics for inspiralling compact binaries with spins at the fourth post-Newtonian order, J. Cosmol. Astropart. Phys. 09 (2021) 029.
[73] A. Antonelli, C. Kavanagh, M. Khalil, J. Steinhoff, and J. Vines, Gravitational Spin-Orbit Coupling Through Third-Subleading Post-Newtonian Order: From First-Order

Self-Force to Arbitrary Mass Ratios, Phys. Rev. Lett. **125**, 011103 (2020).

[74] A. Antonelli, C. Kavanagh, M. Khalil, J. Steinhoff, and J. Vines, Gravitational spin-orbit and aligned $\text{spin}_1 - \text{spin}_2$ couplings through third-subleading post-Newtonian orders, Phys. Rev. D **102**, 124024 (2020).

[75] M. Khalil, Gravitational spin-orbit dynamics at the fifth-and-a-half post-Newtonian order, Phys. Rev. D **104**, 124015 (2021).

[76] Z. Liu, R. A. Porto, and Z. Yang, Spin effects in the effective field theory approach to post-Minkowskian conservative dynamics, J. High Energy Phys. 06 (2021) 012.

[77] D. Kosmopoulos and A. Luna, Quadratic-in-spin Hamiltonian at $\mathcal{O}(G^2)$ from scattering amplitudes, J. High Energy Phys. 07 (2021) 037.

[78] H. Tagoshi, M. Shibata, T. Tanaka, and M. Sasaki, Post-Newtonian expansion of gravitational waves from a particle in circular orbits around a rotating black hole: Up to $O(v^8)$ beyond the quadrupole formula, Phys. Rev. D **54**, 1439 (1996).

[79] S. Akcay, S. R. Dolan, C. Kavanagh, J. Moxon, N. Warburton, and B. Wardell, Dissipation in extreme-mass ratio binaries with a spinning secondary, Phys. Rev. D **102**, 064013 (2020).

[80] Please see Supplemental Material at http://link.aps.org/supplemental/10.1103/PhysRevD.106.L101501 for detailed expressions of the coefficients entering the binding energy and GW flux.

[81] A. Nagar, F. Messina, P. Rettegno, D. Bini, T. Damour, A. Geralico, S. Akcay, and S. Bernuzzi, Nonlinear-in-spin effects in effective-one-body waveform models of spin-aligned, inspiralling, neutron star binaries, Phys. Rev. D **99**, 044007 (2019).

[82] M. Boyle, D. A. Brown, L. E. Kidder, A. H. Mroue, H. P. Pfeiffer, M. A. Scheel, G. B. Cook, and S. A. Teukolsky, High-accuracy comparison of numerical relativity simulations with post-Newtonian expansions, Phys. Rev. D **76**, 124038 (2007).

[83] L. Blanchet, Innermost circular orbit of binary black holes at the third post-Newtonian approximation, Phys. Rev. D **65**, 124009 (2002).

[84] E. Poisson, Absorption of mass and angular momentum by a black hole: Time-domain formalisms for gravitational perturbations, and the small-hole/slow-motion approximation, Phys. Rev. D **70**, 084044 (2004).

[85] R. A. Porto, Absorption effects due to spin in the worldline approach to black hole dynamics, Phys. Rev. D **77**, 064026 (2008).

[86] W. D. Goldberger, J. Li, and I. Z. Rothstein, Non-conservative effects on spinning black holes from world-line effective field theory, J. High Energy Phys. 06 (2021) 053.

[87] N. T. Maia, C. R. Galley, A. K. Leibovich, and R. A. Porto, Radiation reaction for spinning bodies in effective field theory I: Spin-orbit effects, Phys. Rev. D **96**, 084064 (2017).

[88] N. T. Maia, C. R. Galley, A. K. Leibovich, and R. A. Porto, Radiation reaction for spinning bodies in effective field theory II: Spin-spin effects, Phys. Rev. D **96**, 084065 (2017).

[89] S. Marsat, Cubic order spin effects in the dynamics and gravitational wave energy flux of compact object binaries, Classical Quantum Gravity **32**, 085008 (2015).

[90] J. M. Martín-García *et al.*, xAct: Efficient tensor computer algebra for the wolfram language, www.xact.es (2019).